JOURNAL OF MATERIALS SCIENCE 27 (1992) 3026–3031

Conducting transparent indium–tin oxide films by post-deposition annealing in different humidity environments

N. G. PATEL, B. H. LASHKARI*
*Department of Electronics, Sardar Patel University, and *V. P. and R.P.T.P. Science College, Vallabh Vidyanagar 388120, Gujarat, India*

Indium–tin oxide (ITO) films were grown by the flash evaporation method without oxygen gas flow during deposition. The minimum electrical resistivity and the maximum average optical transmittance were found at the optimized substrate temperature of about 673 K. Further improvements in the electrical conductivity and the optical transmittance of ITO films were made by post-deposition annealing under different conditions of humidity. The effects of post-deposition annealing in the presence of the different conditions of humidity on the electrical as well as the optical properties of ITO films were studied. The values of the intrinsic bandgap and effective mass were calculated. The implications are discussed.

1. Introduction

Thin films of electrically conducting and optically transparent indium–tin oxide (ITO) are being widely studied [1]. They have been used extensively as transparent electrodes in various display devices [2] and heterojunction solar cells [3–5], antireflection coatings for solar cells [6] and heat mirrors [7]. These films have been deposited by a variety of methods, such as chemical vapour deposition [8], spray pyrolysis [9], magnetron sputtering [10], radio-frequency sputtering [11], electron-beam evaporation [12] and direct evaporation [13, 14]. The electrical and optical properties of these films are interrelated and depend on their microstructure, stoichiometry and the nature of the impurity present, which in turn depend on the substrate temperature and oxidation processes that occur during or after deposition. As a result each deposition method has characteristic parameters that must be optimized to yield desirable properties. Keeping in view the work already reported on conducting transparent ITO thin films, the present investigation was aimed at attempting to study the growth of the ITO by the flash evaporation method without the special adjustment of oxygen gas flow in the vacuum chamber, and the effect of post-deposition annealing in the presence of various humid atmospheres on the electrical as well as the optical properties of ITO films.

2. Experimental procedure

2.1. Preparation of films

In order to obtain desirable film properties, cleaning of the substrate surface before film deposition is essential. For this the glass substrates were cleaned by successive immersions in chromic acid and doubly distilled water, and were then ultrasonically cleaned in a detergent solution. After washing with doubly distilled water, they were rinsed with acetone and dried under an electric lamp (100 W). The films of ITO were grown using the flash evaporation technique. The source material was a fine powder of substance A (In_2O_3 + 17% Sn_2O_3, an Alfa product). A vacuum of the order of 10^{-4} Pa was maintained during the deposition of films. The films were grown at different substrate temperatures, ranging from 303 to 723 K. After maintaining a steady substrate temperature, the electrical supply to the tantalum boat was switched on and was increased slowly so that the temperature rose to about 1100 K. Then the electrical supply to the electromagnetic vibrator was switched on slowly so that the fine grains of ITO powder could fall on to the heated tantalum boat and evaporate instantaneously. The thickness of the films was measured using a quartz crystal monitor mounted near to the substrate holder. The rate of deposition of the films was kept constant at about 4–7 nm s^{-1}. The film thickness was maintained at about 300 nm for all sets of experimental observations.

In order to study the effects of the substrate temperature on the electrical resistivity and optical transmittance, the samples were prepared under identical conditions by keeping all other deposition parameters constant. The measurements of the electrical resistivity were carried out at room temperature and in the atmosphere using the standard four-probe method. Silver pasted leads were used as a contact to the films. A Specord ultraviolet–visible spectrophotometer was used to study the transmission spectra and optical absorption.

0022–2461 © 1992 Chapman & Hall

2.2. Post-deposition annealing of ITO films under different humid conditions

Fig. 1 is a schematic diagram of post-deposition annealing of ITO films in the furnace at different values of relative humidity (RH). The method of introducing humidity into the furnace tube during annealing of ITO films is commonly used when water is the oxidizing species. In this method air slowly enters the inlet side of the bubbler, becomes saturated with distilled water as it rises through the water and then exits through the outlet into the furnace. The RH is controlled by controlling either the temperature of the air that enters the inlet of the bubbler or the temperature of the water in the bubbler. In the first case the control of humidity is easy, whereas the second case requires more attention for controlling the humidity for two reasons: maintenance of a constant temperature is important because the vapour pressure of water varies with temperature, and it is necessary to prevent any condensation of vapour in the outlet tube of the bubbler by cooling.

Apart from the above method, the ITO films can also be annealed at different values of RH of the environment, but require 20–25 min additional annealing time.

3. Results and discussion

3.1. Effect of the substrate temperature on the electrical resistivity and the optical transmittance

The variation of the electrical resistivity, ρ, of ITO films of thickness 300 nm with the substrate temperature, T_s, is shown in Fig. 2. It is observed that the electrical resistivity decreases with increasing substrate temperature and reaches a minimum value of about $3 \times 10^{-3}\ \Omega$cm at 673 K. This decrease in resistivity can be explained using the Petritz barrier model [15]. Since the crystallites do not grow sufficiently large at low temperatures, the intercrystalline regions are wide, offering a high resistance to the motion of charge carriers. At higher substrate temperatures the formation of fewer nucleation centres results in large crystallite sizes that ultimately decrease the intercrystalline barriers. The charge carriers therefore have to cross comparatively narrow intercrystalline barriers and this may be responsible for the decrease in the resistivity. Dutta and Ray [16] reported that the electrical resistivity of ITO films deposited without any oxygen gas flow in the chamber decreases with increasing substrate temperature, due to the improvement in the crystallinity of the films.

It is also observed from Fig. 2 that the electrical resistivity of the ITO films deposited above $T_s = 673$ K increases. This increase may be attributed to an improvement in the stoichiometry and/or contamination of ITO films by alkali ions of the glass substrate. The improvement in stoichiometry of the oxide semiconductor thin films leads to an increase in the electrical resistivity [17]. Manifacier *et al.* [18] reported that the diffusion of alkali ions from the glass substrate to the ITO film takes place at high deposition temperature. The alkali cations act as p-type doping agents and compensate the native donors. Hence, this increases the electrical resistivity of ITO films. It was observed in the present study that the possibility of contamination can be minimized by the deposition of an interfacial layer of silicon monoxide (SiO) between ITO and the glass substrate. However, in such a case the electrical resistivity of the ITO films retains the higher value. These observations lead to the conclusion that the increase in electrical resistivity above 673 K is due only to an improvement in the stoichiometry.

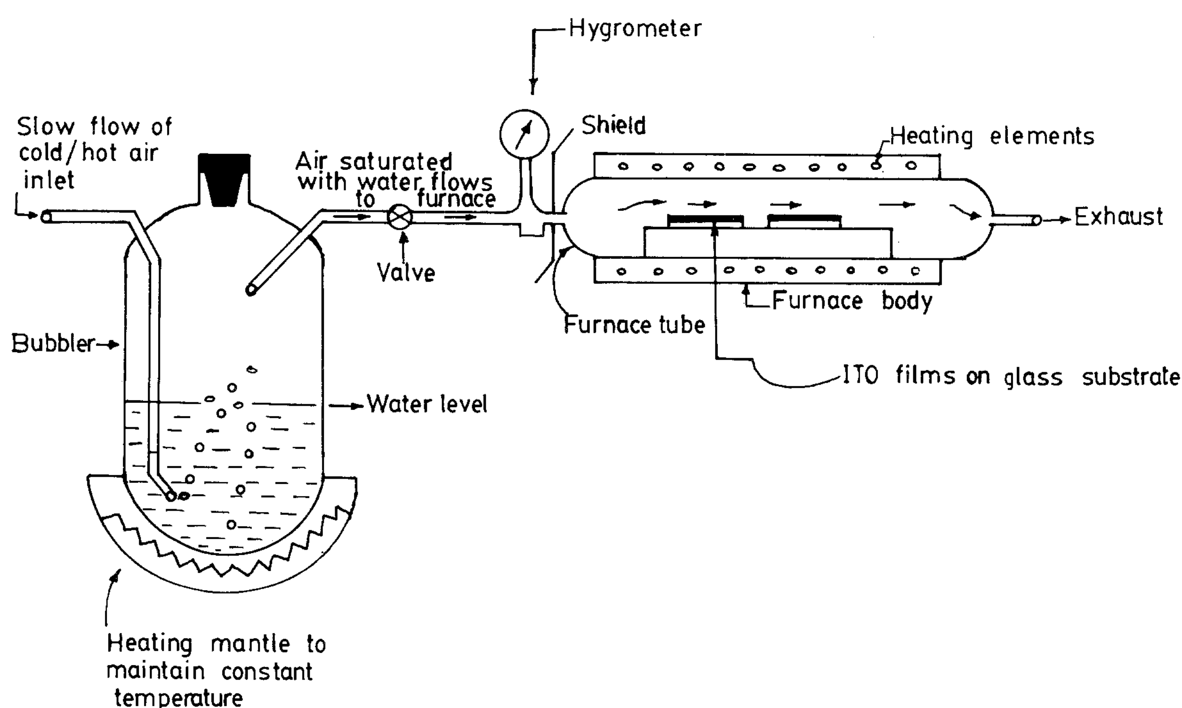

Figure 1 Schematic diagram of post-deposition annealing of ITO films in the presence of atmospheres of different humidity.

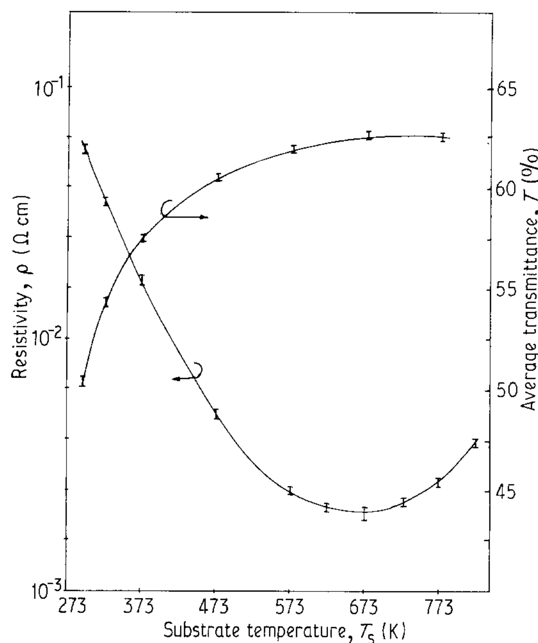

Figure 2 Variation of the electrical resistivity and the average optical transmittance in the visible region with the substrate temperature.

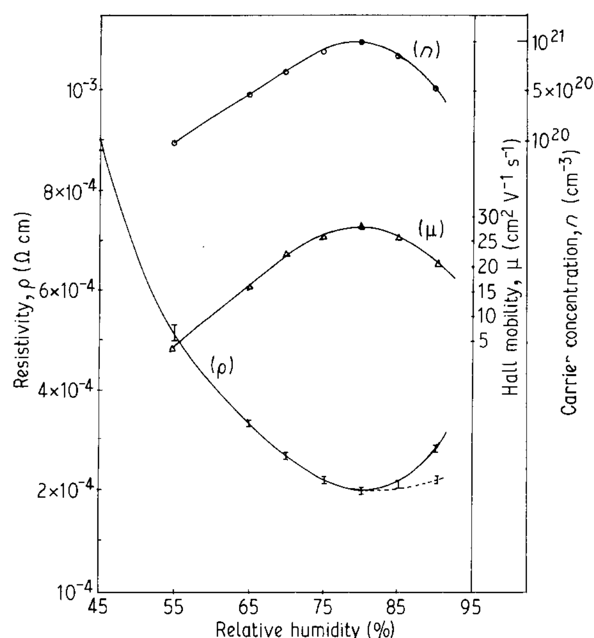

Figure 3 Variation of the electrical resistivity, carrier concentration and mobility with RH during the annealing of ITO films.

The optical absorption is the next important property of thin films of oxide semiconductors. The variation of the average percentage values of transmittance, T, in the visible region with the substrate temperature, T_s, is also shown in Fig. 2. It is observed that the average percentage values of transmittance in the visible range increase with increasing substrate temperature up to 673 K and then saturate. This is due to the decrease in the degree of roughness that developed on the surface of the films and the density of structural defects in the films deposited at higher substrate temperatures, which causes less light scattering so the optical transmission is increased. Dutta and Ray [16] also observed a similar variation of T with T_s in ITO films deposited by magnetron sputtering.

Thus, it is concluded from Fig. 2 that ITO films deposited without any oxygen gas flow in the vacuum chamber have a minimum electrical resistivity of about 3×10^{-3} Ω cm and the average transmittance in the visible region is about 63% at a substrate temperature of about 673 K. In order to further minimize the electrical resistivity and improve the value of T, the ITO films were annealed under different conditions of humidity. The annealing temperature was kept constant at about 700 K and the annealing time was about 40 min.

3.2. Effect of percentage relative humidity during annealing on the electrical resistivity, mobility and carrier concentration

The variation of the electrical resistivity, ρ, mobility, μ, and carrier concentration, n, of ITO films deposited at $T_s = 673$ K for different percentage values of humidity during annealing are shown in Fig. 3. It is observed that the resistivity decreases with increasing humidity and reaches a minimum value of 2×10^{-4} Ω cm at about 80% RH. This may be due to higher humidity providing more available oxygen to the ITO films during annealing. The substitutional incorporation of tin up to a certain level in the films increases with the increase of oxygen from the increased humidity, which leads to an increase of the free-electron density and donor action.

It is also observed from Fig. 3 that the presence of humidity higher than 80% increases the resistivity of ITO films due to the following possibilities.

1. Substitutional incorporation of a higher tin concentration in the films in the presence of higher humidity leads to a decrease in free charge carriers. Kostlin *et al.* [19] pointed out that a tin ion that is surrounded by In_2O_3 can act as a donor, but if one of the nearest-neighbour sites around this primary tin is also filled with a second tin ion their donor action is compensated. Hence, the resistivity of a film increases.
2. Resistivity could increase due to the possible formation of phases such as SnO and Sn_3O_4 at higher humidity. Fan and Goodenough [20] reported such phases in ITO films in the presence of higher oxygen partial pressure.
3. The number of oxygen vacancies probably decreases in an atmosphere of higher humidity. Oxygen may diffuse into the grain boundaries and cause an increase in barrier height as suggested by Shanti *et al.* [21]. This increase in the grain boundary potential consequently increases the resistivity.

It was observed in the present study that when the films annealed above 80% RH were subjected to a reduction process, i.e. further annealed at 723 K in a vacuum of 10^{-4} Pa for 1 h, the resistivity of the films decreased, which may have been due to the fact that during heat treatment in the presence of vacuum the rate of diffusion of excess gas molecules out of the film

increases and thus the resistivity decreases, an effect also shown in Fig. 3 by the broken curve. Dietrich *et al.* [22] reported that almost all of the excess oxygen is removed from the ITO films during heat treatment in high vacuum. Similarly, the mobility and carrier concentration continue to increase as the humidity increases, until their maximum values are reached at 80% RH, after which both the mobility and carrier concentration start to decrease as the humidity increases further. The increases in mobility and carrier concentration are due to the substitutional incorporation of tin in the films, which increases with increasing humidity. The addition of tin liberates many carriers at first, but further addition inevitably causes disorder in the In_2O_3 lattice. Disorder enhances the scattering mechanisms, such as phonon scattering and ionized impurity scattering, resulting in a decrease in mobility. A lattice distorted too much in this way can no longer be effective either in generating Sn^{4+} ions on the substitutional sites in In^{3-} or in generating "effective" oxygen vacancies. The number of free carriers, and hence the carrier concentration, decreases sharply for a relative humidity of more than 80%.

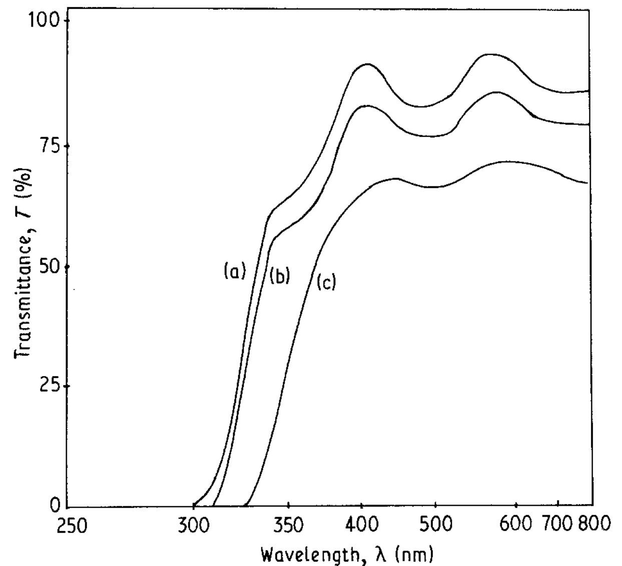

Figure 4 Transmittance spectra for ITO films on glass substrate: (a) 80%, (b) 70% and (c) 55% RH during annealing.

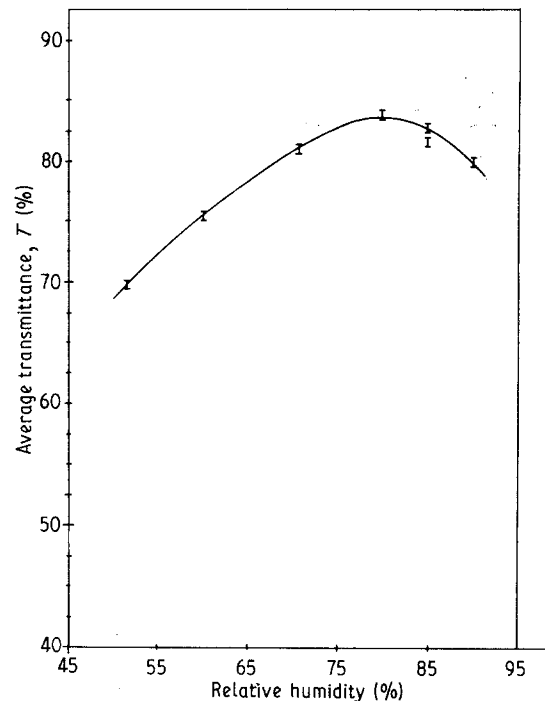

Figure 5 Variation of the average optical transmittance in the visible region with RH.

3.3. Effect of relative humidity on the optical properties

The transmittance spectra for ITO films are shown in Fig. 4. The visible region is almost optically transparent for these films. The transmission of light in this region is limited by several factors: absorption (about 1–2%) in the films [23, 24], which is primarily due to free carriers; backwards scattering (about 1–2%), which is primarily due to surface roughness and increases with increasing thickness [25]; and forwards scattering (about 3%), which is due to inhomogeneities in the film in the form of unreacted or partly reacted chemical species generated during the complex pyrolytic process, segregated atoms, trapped gases or other oxide phases.

The average transmittance in the visible region was determined from Fig. 4. The variation of the average transmittance in the visible range with RH during annealing was plotted and is shown in Fig. 5. It is observed that the average transmittance increases up to 84% with increasing RH up to 80%. This is due to improvement in the carrier concentration. A further increase in RH decreases the average transmittance. This is due to the formation of some metallic clusters or some complex oxide phases in the films. The light scattering from these clusters decreases the transmittance.

It is also observed from Fig. 4 that the sharp decrease in the transparency of the films in the ultraviolet region is caused by a fundamental light absorption by charge carriers. The absorption coefficient, α, which depends on the wavelength, λ, can be obtained by using the Moss [26] relationship

$$T_\lambda = (1 - R_\lambda)^2 \exp(-\alpha_\lambda d) \quad (1)$$

where T_λ is the transmittance, R_λ is the reflectance, α_λ is the absorption at a particular wavelength λ and d is the film thickness. If we neglect the reflection loss, Equation 1 becomes

$$T_\lambda = \exp(-\alpha_\lambda d) \quad (2)$$

This can be simplified to

$$\alpha_\lambda = (2.303/d)\log_{10} T_\lambda^{-1} \quad (3)$$

The transmittance in the ultraviolet–visible region has been measured for a film thickness of about 300 nm. Using Equation 3 the absorption coefficients for different energies were calculated. The dependence of α on the photon energy $h\nu$, where ν is the wave number and h is Planck's constant, was found to obey a

relation of Moss [26]

$$\alpha = A(h\nu - E_g)^{1/2} \quad (4)$$

which is valid for the allowed direct transitions. It is clear from Equation 4 that the graph drawn between α^2 and photon energy ($h\nu$) will be a straight line and its intercept on the $h\nu$-axis will give the optical energy gap E_g. Such experimental plots for different RH values during annealing are shown in Fig. 6. When the straight-line portion of these plots is extrapolated to $\alpha = 0$ the direct optical energy gap, E_g, can be determined. These were found to be 3.75, 3.97, 4.05 and 4.165 eV for 55, 90, 70 and 80% RH present during annealing of ITO films, respectively. These values are listed in Table I.

It is observed from Table I that the optical energy bandgap $(E_g)_{opt}$ increases as the RH increases up to 80%. The optical energy bandgap of ITO film is shifted to higher energies (i.e. shorter wavelengths) due to the increase in carrier concentration with increasing RH up to 80%. This effect can be interpreted as a Moss–Burstein shift [26, 27]. This shift is due to the filling of the states near the bottom of the conduction

TABLE I Effect of percentage RH on the carrier concentration $(E_g)_{opt}$ and $(\Delta E_g)_{MB}$

Relative humidity (%)	Carrier concentration n (cm^{-3})	$n^{2/3}$ ($10^{14}\,cm^{-2}$)	$(E_g)_{opt}$ (eV)	$(\Delta E_g)_{MB}$ (eV)
55	10^{20}	0.215	3.75	0.10
70	7×10^{20}	0.789	4.05	0.40
80	10^{21}	1.000	4.165	0.515
90	5×10^{20}	0.626	3.97	0.320

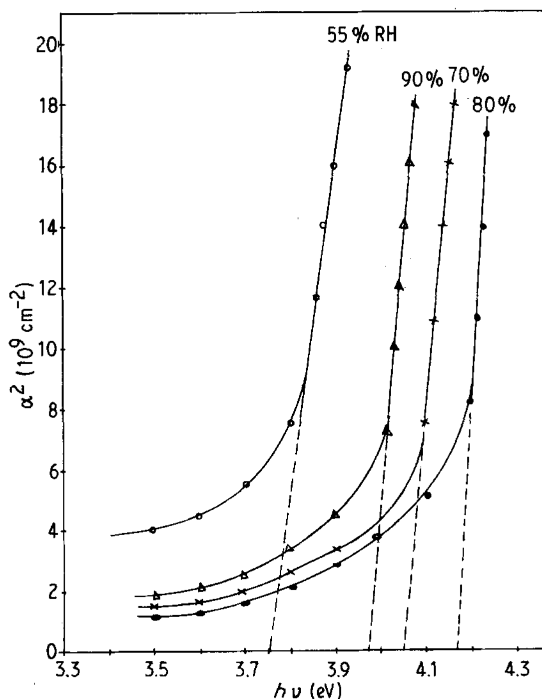

Figure 6 Plot of α^2 versus $h\nu$ for ITO films annealed in the presence of different humidities.

band. A further increase in RH above 80% decreases $(E_g)_{opt}$, due to the decrease in carrier concentration.

The measured bandgap at a carrier concentration n is given by

$$(E_g)_{opt} = (E_g)_{int} + (\Delta E_g)_{MB} \quad (5)$$

where $(E_g)_{int}$ is the intrinsic bandgap and $(\Delta E_g)_{MB}$ is the Moss–Burstein shift or widening. Assuming parabolic band edges, $(\Delta E_g)_{MB}$ can be described in the same way as the Fermi energy of a free-electron gas [19]

$$(\Delta E_g)_{MB} = \frac{h^2}{8m^*_{vc}}\left(\frac{3n}{\pi}\right)^{2/3} \quad (6)$$

where m^*_{vc} is the conduction band effective mass, which also includes the contribution from the valence band curvature. From the above equations it is clear that $(E_g)_{opt}$ is directly proportional to $n^{2/3}$.

A plot of $(E_g)_{opt}$ versus $n^{2/3}$ is shown in Fig. 7. The straight-line nature of the plot is in good agreement with the Moss–Burstein effect. When a straight line is extrapolated to the energy axis it gives the value of intrinsic bandgap $(E_g)_{int}$ of the ITO films. This value was found to be 3.65 eV, which is in close agreement with the value of 3.6 eV reported by Bosnell and Waghorne [28] and Shewchum *et al.* [29].

Using $(E_g)_{int} = 3.65$ eV and Equation 5, $(\Delta E_g)_{MB}$ was calculated and is also shown in Table I. A plot of $(\Delta E_g)_{MB}$ versus $n^{2/3}$ is also shown in Fig. 7. The nature of the plot is a straight line. The experimental points fit the $n^{2/3}$ dependence, confirming the assumption of parabolic band edges. The slope of this plot gives a value of $m^*_{vc} = 0.525m_e$ (where m_e is the rest mass of the electron), which is similar to the value of $0.58m_e$ quoted by Kostlin *et al.* [19].

4. Conclusion

ITO films deposited without oxygen gas flow in the chamber during deposition at the optimized substrate temperature have a minimum electrical resistivity of about $3\times10^{-3}\,\Omega$cm and maximum average optical transmittance of about 63%. Using a simple and inexpensive method of post-deposition annealing in

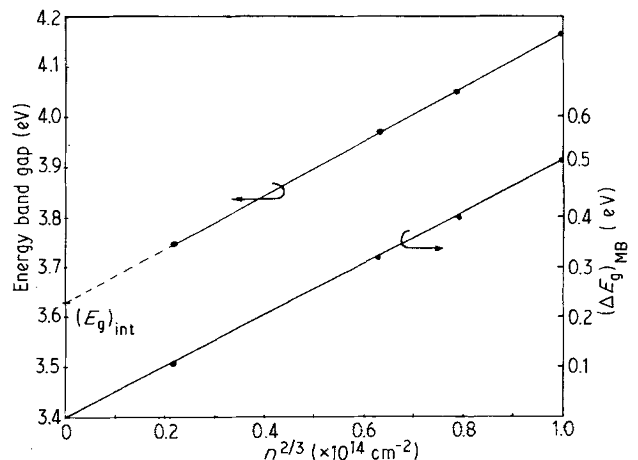

Figure 7 Plots of optical energy bandgap and Moss–Burstein widening $(\Delta E_g)_{MB}$ as a function of $n^{2/3}$.

the presence of 80% RH, ITO films have a minimum electrical resistivity of about $2 \times 10^{-4}\ \Omega$cm and a maximum average optical transmittance of about 84%. The variation of the optical energy bandgap with the carrier concentration obeys the Moss–Burstein widening effect. The values of intrinsic bandgap $(E_g)_{int}$ and effective mass, m^*_{vc}, are nearly in agreement with the reported values.

References

1. K. L. CHOPRA, S. MAJOR and D. K. PANDYA, *Thin Solid Films* **102** (1983) 1.
2. J. Z. PANKOVA (editor), "Display devices", Topics in Applied Physics, Vol. 40 (Springer-Verlag, Berlin, 1980).
3. J. C. MANIFACIER, L. SZEPESSY, L. F. BRESSE, M. PEROTIN and R. STUCK, *Mater. Res. Bull.* **14** (1979) 163.
4. A. BANERJEE, S. R. DAS, A. P. THAKOOR, H. S. RANDHAWA and K. L. CHOPRA, *Solid-St. Elec.* **22** (1979) 495.
5. D. E. CARLSON, in Proceedings of the 14th IEEE Photovoltaic Specialists Conference, San Diego, California, 1980 (Institute of Electrical and Electronic Engineers, New York, 1980) p. 291.
6. I. CHAMBOULEYRON and E. SAUCEDO, *Sol. Energy Mater.* **1** (1979) 299.
7. C. M. LAMPERT, *ibid.* **6** (1981) 1.
8. J. KANE, H. P. SCHWEIZER and W. KERN, *Thin Solid Films* **29** (1975) 155.
9. J. C. MANIFACIER and J. P. FILLAND, *ibid.* **77** (1981) 67.
10. M. BUCHANAN, J. B. WEBB and D. F. WILLIAMS, *Appl. Phys. Lett.* **37** (1980) 213.
11. J. C. C. FAN, F. J. BANCHNER and G. H. FOLEY, *ibid.* **31** (1977) 773.
12. A. HJORTSBERG, I. HAMBERG and C. G. GRANQVIST, *Thin Solid Films* **90** (1982) 323.
13. M. MIZUHASHI, *ibid.* **70** (1980) 91.
14. I. HAMBERG, and C. G. GRANQVIST, *J. Appl. Phys.* **60** (1986) R 123.
15. R. L. PETRITZ, *Phys. Rev.* **104** (1956) 1508.
16. J. DUTTA and S. RAY, *Thin Solid Films* **162** (1988) 119.
17. P. KOFSTAD, "Nonstoichiometry, diffusion and electric conductivity in binary metal oxides" (Wiley, New York, 1972).
18. J. C. MANIFACIER, L. SZEPESSY, J. F. BRESSE and M. PEROTIN, *Mater. Res. Bull.* **14** (1979) 109.
19. H. KOSTLIN, R. JOST and W. LEMS, *Phys. Status Solidi* (*a*) **29** (1975) 87.
20. J. C. C. FAN and J. B. GOODENOUGH, *J. Appl. Phys.* **48** (1977) 3524.
21. E. SHANTI, A. BANERJEE, V. DUTTA and K. L. CHOPRA, *ibid.* **53** (1982) 1615.
22. A. DIETRICH, K. SCHMALZBAUER, J. SZCZYRBOWSKI and H. HOFFMANN, *Thin Solid Films* **122** (1984) 19.
23. J. C. MANIFACIER, *ibid.* **90** (1982) 297.
24. I. HAMBERG, A. HJORTSBERG and C. G. GRANQUIST, *Proc. Soc. Photo-Opt. Instrum. Engng* **324** (1982) 32.
25. R. POMMIER, C. GRIL and J. MARUCHHI, *Thin Solid Films* **77** (1981) 91.
26. T. S. MOSS, "Optical properties of semiconductors" (Butterworths, London, 1959).
27. E. BURSTEIN, *Phys. Rev.* **93** (1954) 632.
28. J. R. BOSNELL and R. WAGHORNE, *Thin Solid Films* **15** (1973) 141.
29. J. SHEWCHUM, D. BURK, R. SINGH, M. SPITZER and J. DUBOW, *J. Appl. Phys.* **50** (1979) 6524.

Received 6 February
and accepted 12 September 1991